

# Anion-Based Self-assembly of Resorcin[4]arenes and Pyrogallol[4]arenes

Monika Chwastek, Piotr Cmoch, and Agnieszka Szumna\*



Cite This: *J. Am. Chem. Soc.* 2022, 144, 5350–5358



Read Online

ACCESS |



Metrics & More

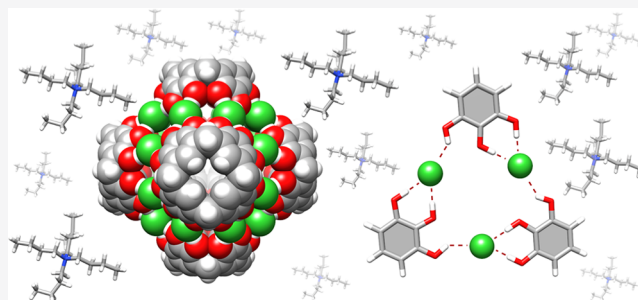


Article Recommendations



Supporting Information

**ABSTRACT:** Spatial sequestration of molecules is a prerequisite for the complexity of biological systems, enabling the occurrence of numerous, often non-compatible chemical reactions and processes in one cell at the same time. Inspired by this compartmentalization concept, chemists design and synthesize artificial nanocontainers (capsules and cages) and use them to mimic the biological complexity and for new applications in recognition, separation, and catalysis. Here, we report the formation of large closed-shell species by interactions of well-known polyphenolic macrocycles with anions. It has been known since many years that C-alkyl resorcin[4]arenes (**R4C**) and C-alkyl pyrogallol[4]arenes (**P4C**) narcissistically self-assemble in nonpolar solvents to form hydrogen-bonded capsules. Here, we show a new interaction model that additionally involves anions as interacting partners and leads to even larger capsular species. Diffusion-ordered spectroscopy and titration experiments indicate that the anion-sealed species have a diameter of >26 Å and suggest stoichiometry  $(M)_6(X^-)_{24}$  and tight ion pairing with cations. This self-assembly is effective in a nonpolar environment (THF and benzene but not in chloroform), however, requires initiation by mechanochemistry (dry milling) in the case of non-compatible solubility. Notably, it is common among various polyphenolic macrocycles (**M**) having diverse geometries and various conformational lability.



## INTRODUCTION

Complexity requires spatial organization. To perform various chemical reactions or physical processes (recognition, separation, and catalysis), nature has evolved compartmentalization strategies that utilize tailored protein cavities or various cellular containers. Chemists, inspired by nature, utilize synthetic building blocks to construct synthetic organizational systems like capsules and cages. Hexameric capsules  $(R_4C)_6(H_2O)_8$  and  $(P_4C)_6$  (Figure 1a,b) are one of the largest and, at the same time, the easiest to obtain artificial capsules based on hydrogen bonds.<sup>1,2</sup> They spontaneously form by interactions between polyphenolic macrocycles [C-alkyl resorcin[4]arenes (**R<sub>4</sub>C**) or C-alkyl pyrogallol[4]arenes (**P<sub>4</sub>C**) Figure 1a,b], enclosing >1000 Å<sup>3</sup> of the internal space. These hexameric capsules (found in the solid state<sup>1,2</sup> and low-polarity solvents<sup>3</sup>) have unique encapsulation properties,<sup>4</sup> exhibit high-fidelity self-sorting,<sup>5</sup> and amazing enzyme-like catalytic activity.<sup>6–8</sup> They are nowadays considered the classics of supramolecular chemistry.<sup>6d,9–12</sup> After many years of extensive studies, it seems that these macrocycles carry no mysteries. However, our recent studies performed for related compounds ([**5**]arenes<sup>13</sup>) demonstrated a new interaction model that has not been known before for polyphenolic macrocycles. It has been found that [**5**]arenes are capable of forming capsules via hydrogen bonds between hydroxyl groups (OH) and anions.<sup>14</sup> These findings inspired us to re-visit interactions between a series of well-known [4]arenes and anions to explore the universal

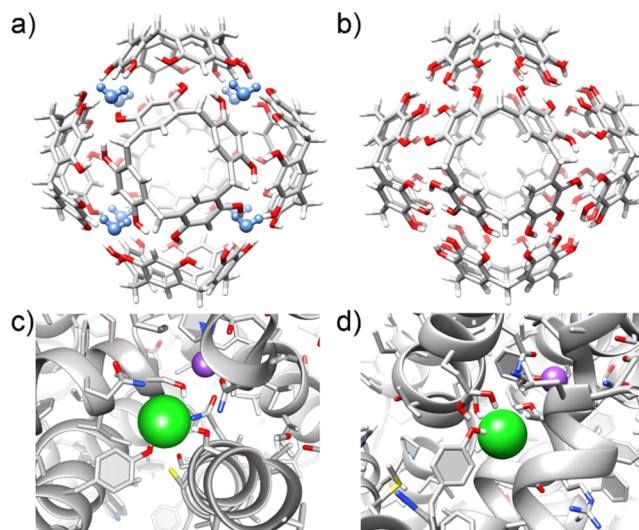


**Figure 1.** State of the art: previously known hexameric capsules (a)  $(R_4C)_6(H_2O)_8$  (ref 1), (b)  $(P_4C)_6$  (ref 2), and (c, d) chloride binding sites found in proteins (refs 15 and 16).

Received: November 15, 2021

Published: March 11, 2022



character of such interactions and test the possibility of the formation of new capsular structures using old building blocks.

The current studies take additional inspiration from the analysis of anion binding sites in proteins (e.g., in chloride-dependent neurotransmitter sodium symporters<sup>15,16</sup>) in which tyrosine or serine (the OH-containing amino acids) are frequently found and OH-anion interactions are common (Figure 1c,d). There is also a growing appreciation of the strength of OH-anion interactions in the field of artificial anion receptors.<sup>17</sup> The non-innocent role of anions during encapsulation of small ammonium cations in dimeric resorcin[4]arene capsules and during interactions between halogenated resorcin[4]arenes and tetraalkylammonium cations has also been noticed by the groups of Rissanen, Bayeh, and Schalley.<sup>18–21</sup> Despite these strong indications, the use of anion-based interactions to assemble polyphenolic macrocycles has been abandoned. In this study, we demonstrate that anion-based self-assembly leads to the formation of large capsular species that possess well-defined structures that are ion-paired with cations. We also show that it is a common phenomenon among many polyphenolic macrocycles (M, Figure 2), involving

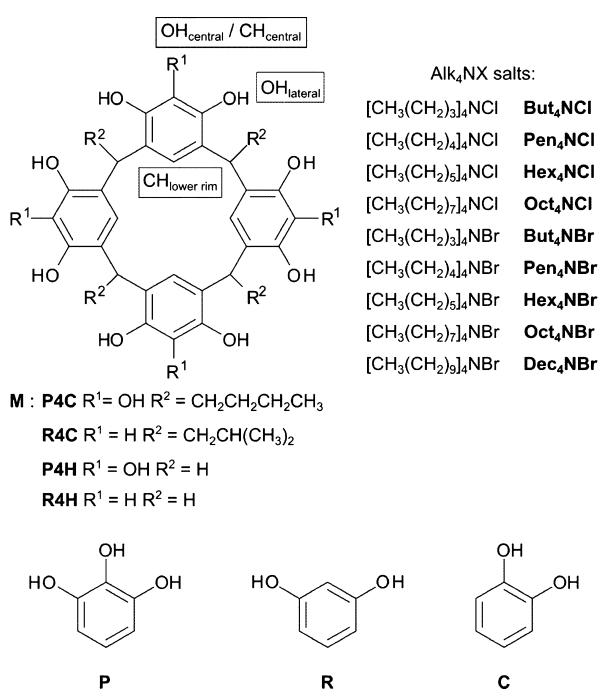


**Figure 2.** Chemical structures of the compounds used in this work and notation of NMR signals.

those containing different substitution patterns and having various conformational lability. Anion-based self-assembly is effective in various media, although, in the case of non-compatible solubility, its initiation requires a non-standard approach (we report here the effectiveness of mechanochemistry).

## RESULTS AND DISCUSSION

**Interactions with Anions in THF.** The interactions between macrocycles (M) and tetraalkylammonium salts which serve as sources of anions (Alk<sub>4</sub>NX, Figure 2) were first studied in THF-*d*<sub>8</sub>. In THF-*d*<sub>8</sub>, contrary to CDCl<sub>3</sub> and benzene, all macrocycles are soluble and exist in monomeric forms, as evidenced from their diffusion coefficients (*D*). Upon addition

of Alk<sub>4</sub>NX, the <sup>1</sup>H NMR signals of upper-rim protons (OH<sub>lateral</sub> and OH<sub>central</sub> for P4C and P4H and OH<sub>lateral</sub> and CH<sub>central</sub> for R4C and R4H) experience substantial downfield shifts ( $\Delta\delta_{\max} \approx +2.5$  ppm, Figure 3a). Although the magnitudes of  $\Delta\delta$  values and the trajectories are different for different macrocycles and salts, in all cases, the magnitudes of  $\Delta\delta$  depend on the type of anion but remain insensitive to the type of cation, indicating that the interactions are dominated by anions. DOSY spectra<sup>22</sup> recorded during titrations show a monotonic increase in the average size of species formed by the macrocycles with borderline values that are similar for all macrocycles (Figure 3c). The size of the species, calculated using the Einstein–Stokes equation from *D* values reached after addition of 8 equiv of the salt (see Supporting Information), corresponds to hydrodynamic diameters  $d_H = 23$  Å for P4H and R4H and  $d_H = 25$  Å for P4C and R4C, where  $d_H = 2r_H$ . In all titration experiments, the plateau is reached at amounts of Alk<sub>4</sub>NX close to 4 equiv per macrocycle.

To suggest a plausible model of interactions between the macrocycles and anions, an analysis of the crystallographic database (CCDC) and a series of DFT calculations were performed (Figure 4a–d).<sup>23</sup> A plot of electrostatic potential (ESP) of the DFT-optimized pyrogallol and resorcinol structures indicates the presence of large clusters of positive ESP along OH-decorated rims, which are responsible for interactions with negatively charged species. Notably, the positive ESP is also present for CH<sub>central</sub> in resorcinol (Figure 4a). In line with these findings, crystal structures retrieved from CCDC demonstrate that resorcin[4]arenes or pyrogallol[4]arenes co-crystallized with Alk<sub>4</sub>NX are surrounded by anions positioned close to their upper rims (various modes, see Figure 4b). However, these CCDC crystal structures were obtained by crystallization from competitive solvents (alcohols) and represent non-discrete structures. Using this structural information, experimental *D* values, and estimated 1:4 stoichiometry, two hypothetical anion-based discrete structures were constructed: tetramer, (M)<sub>4</sub>(X<sup>−</sup>)<sub>16</sub> (Figure S115) and hexamer (M)<sub>6</sub>(X<sup>−</sup>)<sub>24</sub> (Figure 4e,f). The tetramer was excluded due to its small size, exposed charges, and electrostatic repulsions. The hexamer with theoretical  $d_H = 23 \div 25$  Å (the model neglects counterions and a solvation sphere) corresponds quite well to experimental  $d_H = 23$  Å. The internal volume of the hexamer is 1830 Å<sup>3</sup>, which is 40% larger than the internal volume of hydrogen-bonded (P<sub>4</sub>C)<sub>6</sub> (1310 Å<sup>3</sup>). The hexamer is based on a C<sub>4</sub>-crown conformation of P4H, and the binding motif involves the formation of trimeric clusters with anions separated/bridged by OH groups. This binding motif was inspired by the geometry of coordination hexamers,<sup>24</sup> the geometry of anion–water clusters retrieved from CCDC, and it is analogous to the one that has been suggested for [5]arenes.<sup>14</sup> The geometry of the binding motif was optimized using DFT in a vacuum and in THF (continuous solvation model, Figure 4c,d). In a vacuum, geometry optimization of the motif leads to its disintegration due to repulsion between chlorides. On the contrary, in THF, the optimized structure remains hydrogen-bonded with each chloride held by three hydrogen bonds with typical distances, Cl⋯O(H), in the range of 3.1 ÷ 3.3 Å. The Cl⋯Cl distances, which are expected to be repulsive, are 6.2 Å, which are longer than the shortest distances observed for such interactions in the solid state (e.g., in dinuclear oligourea/pyrrole foldamers, Cl⋯Cl = 3.6 ÷ 4.6 Å)<sup>25</sup> and typical for H-separated interchloride distances.

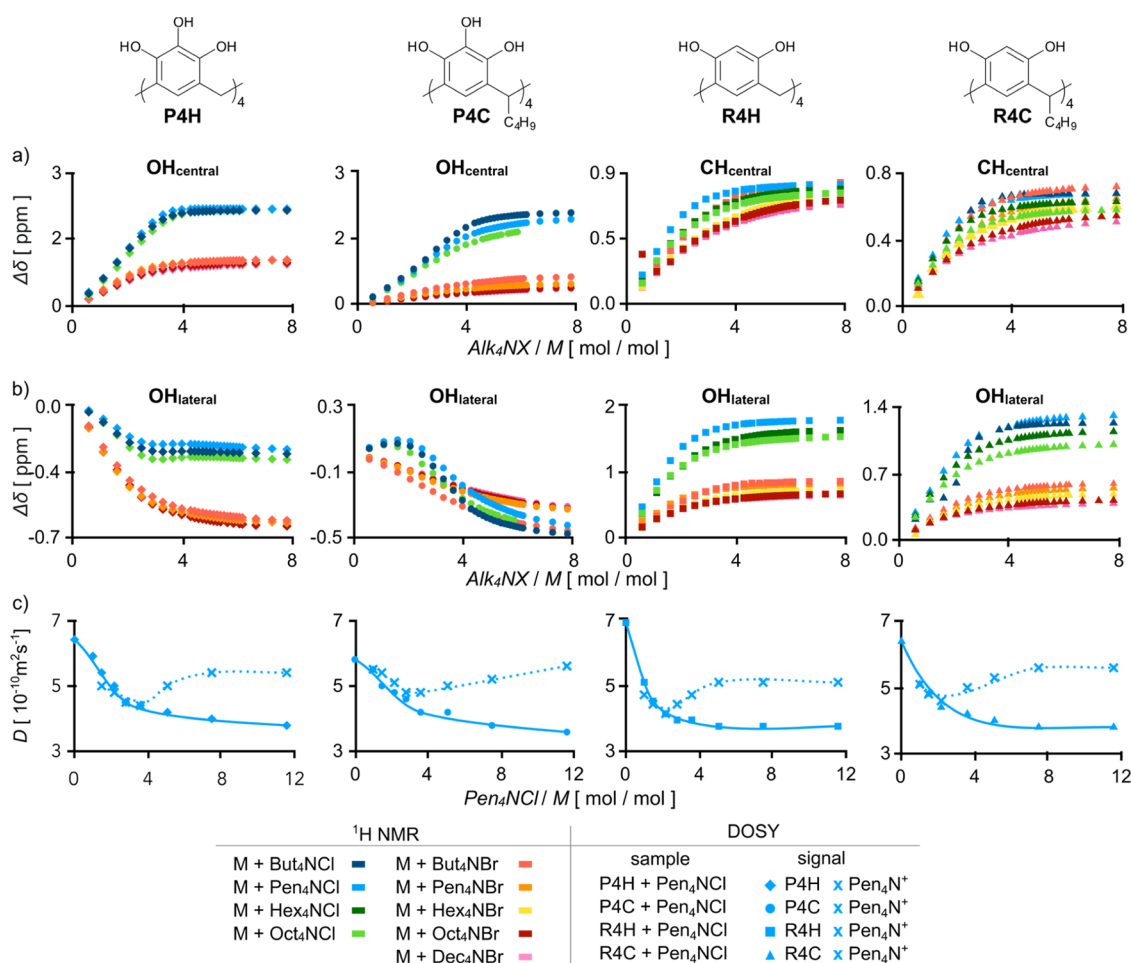
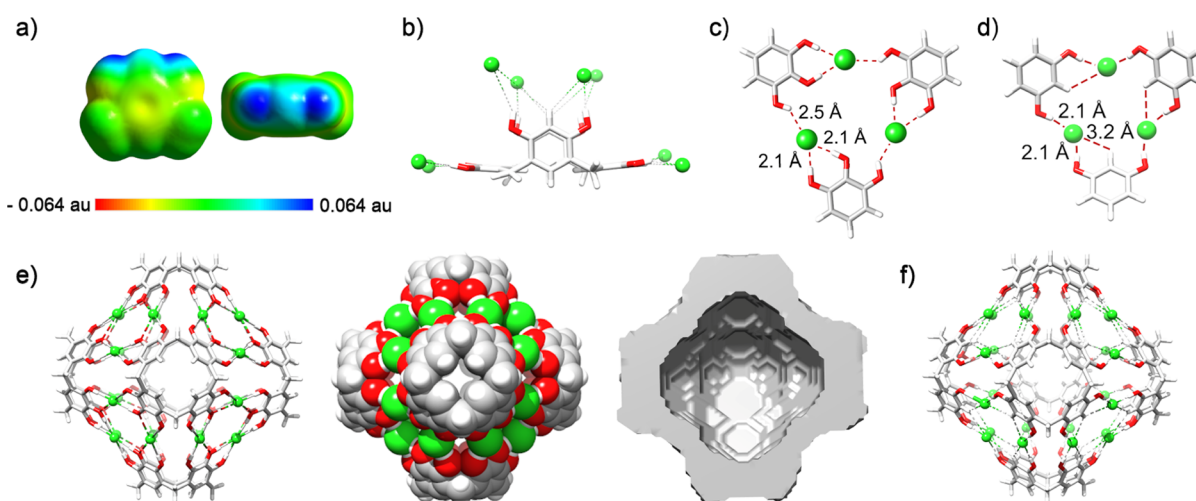


**Figure 3.** <sup>1</sup>H NMR and DOSY titrations of macrocycles (M) P4H, P4C, R4H, and R4C with Alk<sub>4</sub>NX salts in [D<sub>8</sub>]THF: (a) changes in chemical shifts ( $\Delta\delta$ ) for OH/CH central, (b) changes in chemical shifts ( $\Delta\delta$ ) for OH<sub>lateral</sub> and (c) changes of diffusion coefficients ( $D$ ) for signals of M and Alk<sub>4</sub>N<sup>+</sup>. All titrations were performed using solutions of analytes,  $C(M) = 2.5$  mM, and titrant,  $C(M) = 2.5$  mM +  $C(Alk_4NX) = 65$  mM, at 298 K, 600 MHz.



Although the final structure of anion-based species remains uncertain, we think that the model of the hexamer corresponds reasonably well to the experimental data; however, non-

symmetrical structures being in dynamic equilibrium are also possible.

**Interactions with Anions in Benzene.** Expecting that in less polar environments, the anion-sealed capsules may be more

stable (thermodynamically and kinetically), we undertook attempts to obtain anion-sealed capsules in benzene. Without  $\text{Alk}_4\text{NX}$  being added, only **P4C** and **R4C** have detectable solubility in benzene, exhibiting patterns characteristic for  $(\text{P4C})_6$  or  $(\text{R4C})_6(\text{H}_2\text{O})_8$  (Figure 5a,f). With positive experience in the application of mechanochemical ball milling as a method to initialize interaction between the components,<sup>26–29</sup> we used this method to pre-treat the samples.

Macrocycles and the respective salts (1–8 equiv) were dry-milled in a planetary ball mill, and the solids were treated with benzene- $d_6$ . Resorcinarenes (**R4C** or **R4H**) with 1 or 2 equiv of  $\text{Oct}_4\text{NX}$  remained insoluble. However, the addition of 4–8

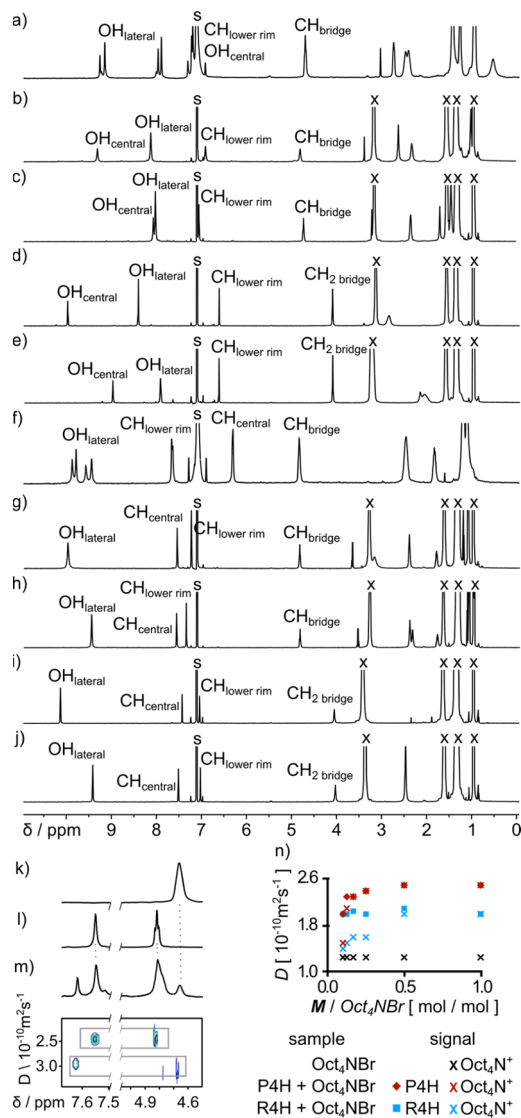


**Figure 5.** Interactions of macrocycles **M** with  $\text{Alk}_4\text{NX}$  in benzene. <sup>1</sup>H NMR spectra for (a)  $(\text{P4C})_6$ , (b) **P4C** +  $\text{Oct}_4\text{NCl}$ , (c) **P4C** +  $\text{Oct}_4\text{NBr}$ , (d) **P4H** +  $\text{Oct}_4\text{NCl}$ , (e) **P4H** +  $\text{Oct}_4\text{NBr}$ , (f)  $(\text{R4C})_6(\text{H}_2\text{O})_8$ , (g) **R4C** +  $\text{Oct}_4\text{NCl}$ , (h) **R4C** +  $\text{Oct}_4\text{NBr}$ , (i) **R4H** +  $\text{Oct}_4\text{NCl}$ , and (j) **R4H** +  $\text{Oct}_4\text{NBr}$  (x— $\text{Oct}_4\text{N}^+$  signals and s—solvent). Partial <sup>1</sup>H NMR spectra for (k)  $(\text{P4C})_6$  and (l)  $(\text{P4C})_6\text{Br}_{24}^-$ , (m) partial <sup>1</sup>H NMR and DOSY spectrum of  $(\text{P4C})_6$  +  $(\text{P4C})_6\text{Br}_{24}^-$ , and (n) changes of diffusion coefficients (*D*) upon variation of the concentration of the macrocycle ( $C(\text{Alk}_4\text{NX})$  40 mM,  $C(\text{M})$  4–40 mM). All samples were prepared mechanochemically and dissolved in  $\text{C}_6\text{D}_6$  (see the experimental part for the procedures, 600 MHz, 298 K).

equiv of  $\text{Oct}_4\text{NX}$  leads to a substantial increase in solubility of **R4C** and **R4H**. Solubility in benzene, especially of the previously insoluble macrocycles, is a strong indication of the formation of closed-shell structures, which engages polar hydroxyl groups and saturates “solvation spheres” of anions. The signals in the <sup>1</sup>H NMR spectra are sharp, and the chemical shifts are anion-dependent but remain insensitive to the cations’ size and the concentration (Figures 5 and S85–S98). The fact that at least 4 equiv of the salt are needed for good solubility supports  $(\text{M})_6(\text{X}^-)_{24}$  stoichiometry. <sup>1</sup>H NMR signals of  $\text{OH}_{\text{lateral}}$  for resorcinarene-based capsules appear at  $\delta \approx 10$  ppm for chlorides and at  $\delta \approx 9.5$  ppm for bromides, reflecting a typical trend and hydrogen bond accepting ability of anions. Particularly notable are the positions of signals of  $\text{CH}_{\text{central}}$  because they move from their typical position at ca  $\delta = 6.4$  ppm (observed, e.g., for  $(\text{R4C})_6(\text{H}_2\text{O})_8$ , Figure 5f) to  $\delta = 7.3$ – $7.6$  and exhibit higher values of  $\delta$  for bromides than for chlorides (Figure 5g,h, a similar trend is also observed during titrations in THF, Figure 3). These downfield shifts indicate that the interactions with anions for resorcinarenes involve not only hydroxyl groups but also  $\text{CH}\cdots$  anion interactions, and these contributions seem to be particularly relevant for interactions with large bromide anions, which is in line with the suggested binding motif.

Pyrogallolarenes (**P4H** and **P4C**) also form anion-sealed capsules in benzene- $d_6$ . **P4H**, initially insoluble in benzene- $d_6$ , becomes soluble (partially or fully) upon the addition of  $\text{Alk}_4\text{NX}$  and mechanochemical pre-treatment. The ratio of **P4H**: $\text{Alk}_4\text{NX}$  in the dissolved part of the sample is at least 1:4, and the chemical shifts remain independent of the various concentrations of the  $\text{Alk}_4\text{NX}$ . The downfield shifts of hydroxyl group signals are consistent with the involvement of all OH groups in hydrogen bonding interactions with anions, with chlorides inducing higher downfield shifts than bromides. **P4C** behaves differently because the **P4C**: $\text{Alk}_4\text{NX}$  ratio in the solution roughly follows the ratio in the solid samples (starts from 1:0.8, not like in previous cases from 1:4). The signals in the <sup>1</sup>H NMR spectrum show concentration-dependent chemical shifts, and the final values of  $\Delta\delta$  are much lower than for complexes of other macrocycles. This indicates that interactions of **P4C** with anions are weaker than those of other macrocycles despite its higher solubility in benzene. Thanks to a stepwise transformation from  $(\text{P4C})_6$  to  $(\text{P4C})_6(\text{Br}^-)_{24}$ , we were able to detect the simultaneous presence of two capsular forms in one sample, and DOSY measurements confirm that the anion-sealed species are larger than neutral hydrogen-bonded capsules (Figure 5k–m).

The crucial role of anions in the self-assembly process was further supported by experiments with salts containing other, non-interacting anions. After mechanochemical pre-treatment of the macrocycles mixed with  $\text{But}_4\text{NF}$ ,  $\text{But}_4\text{NPF}_6$ ,  $\text{But}_4\text{NH}_2\text{PO}_4$ ,  $\text{But}_4\text{NH}_2\text{SO}_3$ ,  $\text{But}_4\text{NNO}_3$ , or  $\text{Pen}_4\text{NI}$  (4 equiv), we found no traces of dissolution of the resulting samples in benzene.

**Role of Cations.** Although self-assembly is predominantly anion-dependent, cationic species are inherently present as counterions.  $\text{Alk}_4\text{N}^+$  can reside either inside or outside the cavity, and due to the dynamic nature of the capsules, they can be in a fast exchange between these positions and various forms of uncompleted species (free or non-specifically aggregated).

<sup>1</sup>H NMR signals of  $\text{Alk}_4\text{N}^+$  undergo upfield shifts upon addition of macrocycles (both in THF- $d_8$  and in benzene- $d_6$ ). For all  $\text{Alk}_4\text{N}^+$ , the largest  $\Delta\delta$  is observed for the methylene protons next to the nitrogen ( $-\text{CH}_2-\text{N}^+$ ,  $\Delta\delta_{\text{max}} \approx -0.48$  ppm,

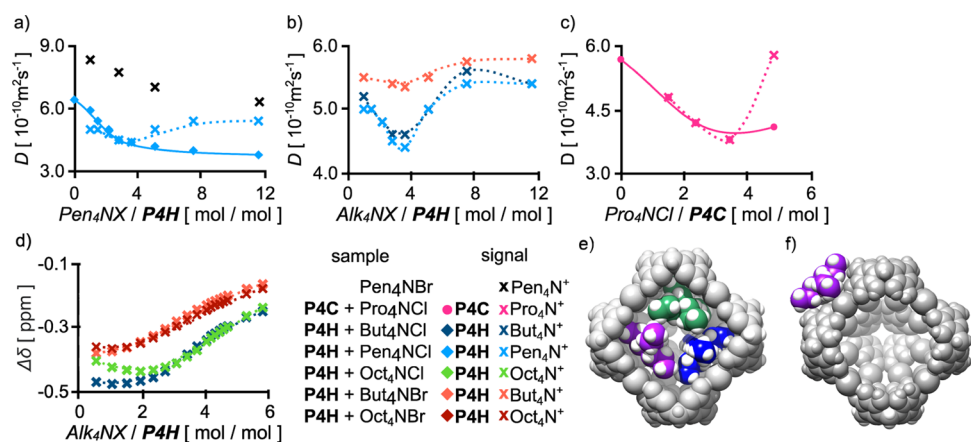


**Figure 6.** Interactions of capsules with cations in  $[\text{D}_8]\text{THF}$ : (a,b) changes in diffusion coefficients ( $D$ ) during the titration of  $\text{P4H}$  with  $\text{Alk}_4\text{NX}$  and a comparison with concentration-dependent changes of  $\text{Pen}_4\text{NBr}$  alone (the same concentration of  $\text{Alk}_4\text{NX}$ ,  $2.5 \div 30 \text{ mM}$ ), (c) diffusion coefficients ( $D$ ) for the samples of  $\text{P4H}$  (mmol) +  $\text{Pro}_4\text{NCl}$  ( $1 \div 5$  equiv), ball-milled and dissolved in  $[\text{D}_8]\text{THF}$ ; the ratio between components was calculated by integration of the spectral (d) changes in  $^1\text{H}$  chemical shifts ( $\Delta\delta$ ) of  $-\text{CH}_2\text{N}^+$  signals during titration of  $\text{P4H}$  with  $\text{Alk}_4\text{NX}$  [all experiments at 298 K, 600 MHz, analyte:  $C(\text{P4H}) = 2.5 \text{ mM}$  and titrant:  $C(\text{P4H}) = 2.5 \text{ mM} + C(\text{Alk}_4\text{NX}) = 65 \text{ mM}$ ]. A model of the anion-sealed capsule with (e) three  $\text{Pro}_4\text{N}^+$  in the cavity, and (f)  $\text{Bu}_4\text{N}^+$  interacting externally (the atoms in the front were partially removed to visualize the interior of the cavity).

Figure 6d), while other signals experience considerably smaller shifts ( $\Delta\delta_{\text{max}} < -0.17 \text{ ppm}$ , Figure S118a). Analysis of  $\Delta\delta$  for various  $\text{Alk}_4\text{NX}$  indicates that the effect of cation size ( $\text{Bu}_4\text{NCl}$  vs  $\text{Oct}_4\text{NCl}$ ) is smaller than the effect of the anion type ( $\text{Alk}_4\text{NCl}$  vs  $\text{Alk}_4\text{NBr}$ ) and chlorides impose larger  $\Delta\delta$  values than bromides (Figure 6d). These properties are interpreted in terms of ion pairing of  $\text{Alk}_4\text{N}^+$  with anion-based capsules (either inside or outside the cavity, Figure 6e,f), which is stronger for capsules containing chlorides than bromides. An upfield shift of  $-\text{CH}_2\text{N}^+$  signals can be explained by electrostatic attractions within an ion pair that change the conformation of  $\text{Alk}_4\text{N}^+$  so that the cationic core is exposed and placed in the proximity of the aromatic walls of the capsules (Figures 6f and S118c).

Ion pairing was also confirmed by DOSY both in  $\text{THF}-d_8$  (Figure 6a,b) and benzene- $d_6$  (Figure 5n). In  $\text{THF}-d_8$ , in the absence of the macrocycles,  $D(\text{Alk}_4\text{N}^+)$  values decrease monotonically with increasing concentration of  $\text{Alk}_4\text{NX}$ , in line with concentration-dependent non-specific aggregation (Figures 6a and S101d). On the contrary, in the presence of the macrocycles, the profiles of changes are substantially different. Upon addition of  $\text{Alk}_4\text{NX}$  to  $\text{M}$  (constant concentration) in  $\text{THF}-d_8$ , the titration curve with respect to  $D(\text{Alk}_4\text{N}^+)$  is non-monotonic (Figure 6a,b). It is interpreted assuming that  $\text{Alk}_4\text{N}^+$  forms an ion pair(s) with a large and highly negatively charged capsule, which leads to a low  $D(\text{Alk}_4\text{N}^+)$  value when the relative concentration of the capsules is high (initial points) and to an increase in the  $D(\text{Alk}_4\text{N}^+)$  value as the amount of  $\text{Alk}_4\text{NX}$  increases. In line with this interpretation,  $D(\text{M})$  values remain at the same level in this experiment and weaker ion pairing with capsules containing  $\text{Br}^-$  leads to less pronounced effects (Figure 6b). In benzene- $d_6$ , non-specific  $\text{Alk}_4\text{NX}$  aggregation is very strong (Figure S116) and the macrocycles have limited solubility. Therefore, the reversed titrations were performed at constant  $\text{Alk}_4\text{NX}$  concentration (Figure 5n). In such a case,  $D(\text{Alk}_4\text{N}^+)$  values are expected to stay constant in absence of specific interactions. However, upon the addition of the macrocycles,  $D(\text{Alk}_4\text{N}^+)$  values systematically increase—up to the values of the postulated anion-sealed capsules. These observations are in line with the hypothesis that cations form ion pairs with large anion-sealed capsules.

To check the possibility of encapsulation of smaller cations,  $\text{Met}_4\text{NX}$ ,  $\text{Et}_4\text{NX}$ , and  $\text{Pro}_4\text{NX}$  were also tested. All these salts are soluble neither in THF nor in benzene. Therefore, the samples containing macrocycles and the respective salts (at a ratio of 1:1 up to 1:8) were ball-milled and subsequently treated with benzene or THF. In benzene, all samples remained insoluble. Quite surprisingly, most of them were also insoluble in THF, even though the macrocycles in their “free” forms were readily soluble in THF. Only  $\text{P4C}/\text{Pro}_4\text{NBr}$  and  $\text{P4C}/\text{Pro}_4\text{NCl}$  were partially dissolved in  $\text{THF}-d_8$  but revealed distinct behaviors. For  $\text{P4C}/\text{Pro}_4\text{NBr}$ , the ratio between dissolved components remains constant, 1:1, irrespective of the initial ratio in the solid sample (Figure S110). Importantly,  $D(\text{Pro}_4\text{N}^+)$  values indicate the formation of small species, most likely by the complexation of cations in the monomeric cavitand. On the contrary, for  $\text{P4C}/\text{Pro}_4\text{NCl}$ , the ratio between dissolved components is variable—from 1:1 to the maximum limiting value of 1:4 (Figure S109). In  $\text{P4C}/\text{Pro}_4\text{NCl}$ , the  $D$  values for the macrocycle and the cation are ratio-dependent and much lower than in  $\text{P4C}/\text{Pro}_4\text{NBr}$ . Particularly striking is the abrupt differentiation of  $D$  values between  $\text{P4C}$  signals and  $\text{Pro}_4\text{N}^+$  signals at the 1:4 ratio (Figure 6c). These data confirm that (1) four  $\text{Cl}^-$  per macrocycle are needed for capsule formation and (2) tight ion pairing involves less than four  $\text{Pro}_4\text{N}^+$  per macrocycle; therefore, at the  $\text{P4C}/\text{Pro}_4\text{NCl}$  1:4 ratio, there is an exchange between “bound” and “free” cations, leading to a higher  $D(\text{Pro}_4\text{N}^+)$  value. Although it is uncertain if the cations reside inside or outside the cavity (or both), our models indicate that three  $\text{Pro}_4\text{N}^+$  cations can fit in the cavity (occupancy 32%), but placing four cations leads to steric hindrance (although possible from the point of view of occupancy). For comparison, the hexameric capsule  $(\text{R4C})_6(\text{H}_2\text{O})_8$  can accommodate two  $\text{Et}_4\text{N}^+$  cations as reported by Cohen.<sup>4f</sup>

Low-temperature experiments for  $\text{P4C}/\text{Pro}_4\text{NCl}$  and  $\text{P4C}/\text{Pen}_4\text{NCl}$  show that within the temperature range  $298 \div 233 \text{ K}$ , the complexes remain dynamic (Figures S119–S122).

**Interactions with Anions in Chloroform.** C-alkyl-substituted macrocycles  $\text{P4C}$  and  $\text{R4C}$  are known to spontaneously and quantitatively form self-assembled capsules  $(\text{R4C})_6(\text{H}_2\text{O})_8$  and  $(\text{P4C})_6$  in chloroform and encapsulate suitably sized  $\text{Alk}_4\text{N}^+$  cations (up to  $\text{Oct}_4\text{N}^+$ ).<sup>4a</sup> It has been

reported that  $\text{Alk}_4\text{NX}$  salts have to be added in small amounts for encapsulation because, otherwise, they induce disassembly.<sup>4a</sup> Here, we evaluate the ability of anions to become components of self-assembled species, and therefore, we used higher amounts of  $\text{Alk}_4\text{NX}$  and systematically screened various [4]arenes by DOSY.

The spectra of **P4C** in chloroform indicate the formation of hexamers ( $\text{P4C}$ )<sub>6</sub>, in line with the previous findings. The addition of  $\text{But}_4\text{NCl}$  leads to the gradual disintegration of the hexamers to monomers, and <sup>1</sup>H NMR spectra show two separate sets of signals having different diffusion coefficients, *D* (Figure 7a). *D* values and chemical shifts for both species remain

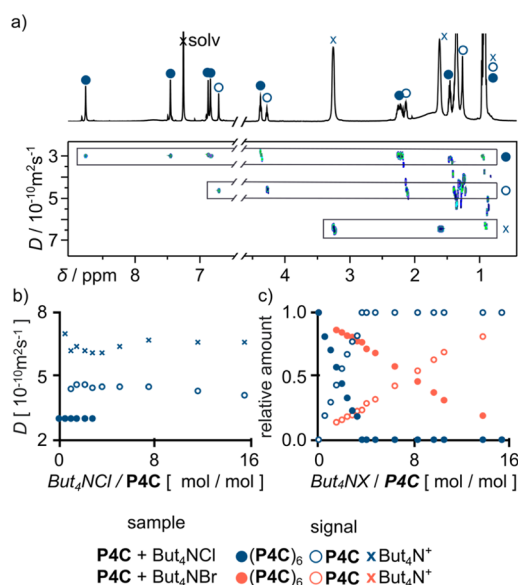


**Figure 7.** Interactions of macrocycles with  $\text{Alk}_4\text{NX}$  in chloroform: (a) <sup>1</sup>H NMR and DOSY spectra of mixture **P4C** (2.5 mM) + **Oct<sub>4</sub>NCl** (65 mM), (b) diffusion coefficients (*D*) for all species during titration of **P4C** with **Oct<sub>4</sub>NCl**, and (c) profiles of the anion-induced disassembly (all in  $\text{CDCl}_3$ , 600 MHz, 298 K).

invariable during the titration (Figure 7b). At 4 equiv of  $\text{But}_4\text{NCl}$  being added, initially formed capsules ( $\text{P4C}$ )<sub>6</sub> are completely disintegrated. Disassembly requires higher amounts of  $\text{But}_4\text{NBr}$  than  $\text{But}_4\text{NCl}$  (Figure 7c), indicating that disassembly is anion-mediated and reflecting a higher hydrogen bonding affinity of chlorides than bromides.

These data demonstrate that in chloroform, interactions between macrocycles and anions are distinctly different than in other solvents: addition of  $\text{Alk}_4\text{NX}$  leads to the disintegration of neutral hydrogen-bonded hexamers and the anion-based capsules are not re-assembled.

**Stability of Complexes.** Due to the complex character of equilibria, various solubility values, and possible cooperative effects, we were not able to determine absolute association constants. However, the relative order of stability can be estimated based on a general rule that, for the same stoichiometry and identical initial concentrations, a stronger interaction gives a stronger curvature of a titration curve.<sup>30</sup> Thus, the data were normalized to the 0–1 range ( $\Delta\delta$  or *D*), and data were analyzed to determine the relative strength of interactions (Figure S103). The plots suggest that for a given macrocycle, the complexes with chlorides are always stronger than those with bromides, which reflects the order of the hydrogen bonding ability of anions. However, the preference toward chlorides is

less pronounced for resorcinarenes than for pyrogallolarenes. This may reflect the particular role of  $\text{CH}\cdots\text{anion}$  interactions for bromides and a good fit between this large anion and a small central atom (here hydrogen, see binding motif). Among the chloride complexes with various macrocycles, the order of stability is as follows: **P4H** > **R4H**  $\approx$  **R4C** > **P4C**. Thus, lower-rim crowded macrocycles are less prone to form complexes, which suggests that some conformational flexibility is required for optimal interactions.

The stability of **P4H**/ $\text{Pen}_4\text{NCl}$  toward the addition of polar solvents was tested by adding water or methanol (0 ÷ 5% vol/vol) to its solution in  $\text{THF-}d_8$ . The addition of polar solvents leads to an increase in *D* values of the components, indicating gradual disassembly (Figure S117). It should be noted that water exerts weaker effects than methanol, when added in the same amounts. The relatively low sensitivity to traces of water in THF (<2%) is also supported by the high reproducibility of the results from experiments performed using different batches of solvent (see Figure S123).

**Role of the Solvent.** The question about the role of the solvent, especially the non-intuitive formation of the complexes in THF but not in less polar chloroform, was posed and theoretically discussed in the previous paper.<sup>14</sup> Here, we evaluated the influence of a solvent on anion binding by using reference non-macrocylic polyphenols—resorcinol (**R**), pyrogallol (**P**), and catechol (**C**). These polyphenols were titrated with  $\text{But}_4\text{NX}$  in  $\text{CDCl}_3$ ,  $\text{THF-}d_8$ , and  $\text{CD}_3\text{CN}$  (Figure 8).

In THF and  $\text{CD}_3\text{CN}$  (used for comparison with the literature),<sup>17</sup> the titration results were fitted using OH signals with 1:1 models (Figure 8a). The association constants (*K*) are

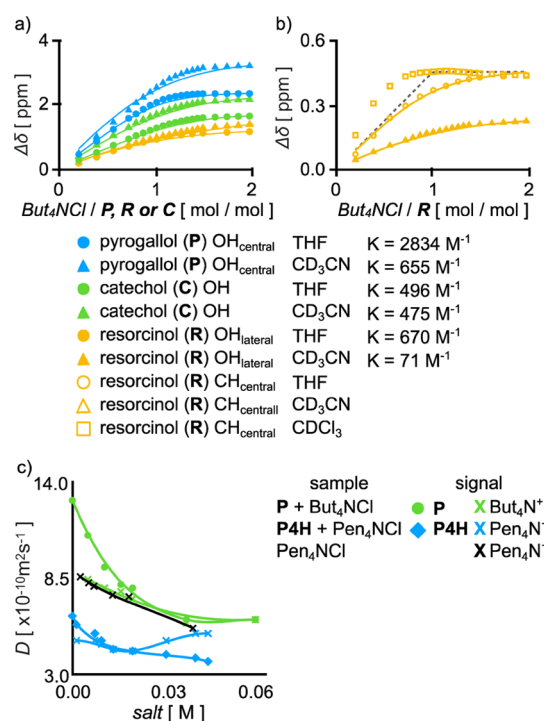


**Figure 8.** <sup>1</sup>H NMR titrations of pyrogallol (**P**), catechol (**C**), and resorcinol (**R**) with  $\text{But}_4\text{NCl}$  in  $\text{CDCl}_3$ ,  $\text{THF-}d_8$ , and  $\text{MeCN-}d_3$ : (a) signals of OH for **P** and **C** and (b) signals of  $\text{CH}_{\text{central}}$  for **R**. Solid lines represent fitted curves and dashed lines represent theoretical curves for the 1:1 model (all experiments at 298 K and 400 MHz). (c) Diffusion coefficients (*D*) for all species during titrations of **P** (10 mM) and **P4H** (2.5 mM) with  $\text{Alk}_4\text{NCl}$ .

considerably higher in THF (reflecting its lower  $\epsilon$ ) than in  $\text{CD}_3\text{CN}$ , and the order of stability is  $\text{P} > \text{R} > \text{C}$ . The formation of complexes in THF was also detected by DOSY (Figures 8c and S125). For example, upon the addition of  $\text{Alk}_4\text{NCl}$  salt, the values of  $D(\text{P})$  decrease to values similar to those of  $D(\text{Alk}_4\text{NCl})$ , reflecting the formation of complexes that have a size similar to the size of the salt itself but smaller than in the case of macrocyclic ligands (Figure 8c). These control experiments explain why macrocyclic compounds, composed of similar phenolic building blocks, also interact with anions in THF.

Determination of stability of anion complexes of **P**, **R**, and **C** in chloroform is difficult due to disappearance of OH signals. Therefore, the comparison between solvents was made only for **R** using its  $\text{CH}_{\text{central}}$  signal (Figure 8b). The shape of the titration curve in  $\text{CDCl}_3$  indicates that interactions between  $\text{Cl}^-$  and **R** are stronger and more complex in  $\text{CDCl}_3$  than in  $\text{THF-}d_8$  and  $\text{CD}_3\text{CN}$  and reflects the coexistence of 2:1, 1:1, and 1:2 complexes (the first maximum is reached before 1 equiv and distinct changes are visible after reaching 2 equiv of the salt). Thus, lack of formation of anion-sealed capsules by macrocyclic compounds in chloroform cannot be attributed solely to weaker interactions between phenolic building blocks and anions in this solvent. Other factors (solvation of the macrocycles, entropic factors, and ion pair formation) have to be further analyzed.

## CONCLUSIONS

The current findings shed new light on the possible modes of interactions between pyrogallol[4]arenes and resorcin[4]arenes with tetralakylammonium salts, pointing out the crucial role of hydrogen bonds with anions. In weakly anion-solvating environments (THF and benzene), anion $\cdots$ OH/CH interactions lead to the formation of large self-assembled capsular species. In sharp contrast, in chloroform, the analogous interactions lead to the destruction of initially formed hexamers and anions do not participate in self-assembly. The newly formed anion-sealed capsules bear a high-density negative charge and form tight but still dynamic ion pairs with cations. These properties are expected to generate unique recognition properties and possibly also catalytic properties. We also think that the ability of resorcinarenes to interact with anionic species may help to understand widely discussed Brønsted acidity of resorcinarene capsules,<sup>6a</sup> unusual selectivity in C–X bond activation,<sup>7a</sup> anion-dependent encapsulations in  $(\text{R4C})_6(\text{H}_2\text{O})_8$  reported by Rebek<sup>4a</sup> or Horiuchi,<sup>51</sup> and the anion-dependent extrusion of water molecules from  $(\text{R4C})_6(\text{H}_2\text{O})_8$  mentioned by Cohen.<sup>4d,f</sup>

Importantly, the current results indicate that the anion-based self-assembly mode is general—it was detected for polyphenolic macrocycles of various ring sizes ([4]arenes and [5]arenes) having different substitution patterns (pyrogallol and resorcinol derivatives) and various levels of conformational rigidity (lower-rim-substituted and unsubstituted derivatives). Thus, we envision that in the future, it can also be found for other polyphenolic macrocycles leading to the discovery of new anion-based closed-shell structures.

## EXPERIMENTAL SECTION

**General Procedure for  $^1\text{H}$  NMR Titrations.** To the solution of a macrocycle ( $C = 0.005$  M, 0.0025 mmol) in  $\text{THF-}d_8$  (0.5 mL), a solution containing  $\text{Alk}_4\text{NX}$  ( $C = 0.075$  M, 0.075 mmol) and the macrocycle ( $C = 0.005$  M, 0.005 mmol) in  $\text{THF-}d_8$  (1 mL) was added in portions.  $^1\text{H}$  NMR spectra were recorded at 303 K using Bruker 400 MHz.

**General Procedure for DOSY Titrations.** To the solution of a macrocycle ( $C = 0.0025$  M, 0.00125 mmol) in  $\text{THF-}d_8$  (0.5 mL), a solution containing  $\text{Alk}_4\text{NX}$  ( $C = 0.0656$  M, 0.0656 mmol) and the macrocycle ( $C = 0.0025$  M, 0.0025 mmol) in  $\text{THF-}d_8$  (1 mL) was added in portions.  $^1\text{H}$  NMR and DOSY spectra were recorded at 303 K using Varian 600 MHz.

**Preparation of the Samples by Mechanochemistry.** Solid sample of a macrocycle (0.01 mmol) and  $\text{Alk}_4\text{NX}$  (1 ÷ 8 equiv) were ball-milled for 1 h in a planetary ball mill. Then, the powder was dissolved in benzene- $d_6$  (0.7 mL). The sample was filtered, and the solution was analyzed by NMR.

## ASSOCIATED CONTENT

### Supporting Information

The Supporting Information is available free of charge at <https://pubs.acs.org/doi/10.1021/jacs.1c11793>.

Experimental details, NMR and DOSY titration curves, and numerical values (PDF)

Atomic coordinates of a hexamer cage (**P4H**)<sub>6</sub>Cl<sub>24</sub> (PDB)

Atomic coordinates of a hexamer cage (**R4H**)<sub>6</sub>Cl<sub>24</sub> (PDB)

## AUTHOR INFORMATION

### Corresponding Author

Agnieszka Szumna — Institute of Organic Chemistry, Polish Academy of Sciences, 01-224 Warsaw, Poland; [orcid.org/0000-0003-3869-1321](https://orcid.org/0000-0003-3869-1321); Email: [agnieszka.szumna@icho.edu.pl](mailto:agnieszka.szumna@icho.edu.pl)

### Authors

Monika Chwastek — Institute of Organic Chemistry, Polish Academy of Sciences, 01-224 Warsaw, Poland

Piotr Cmoch — Institute of Organic Chemistry, Polish Academy of Sciences, 01-224 Warsaw, Poland; [orcid.org/0000-0002-8413-9290](https://orcid.org/0000-0002-8413-9290)

Complete contact information is available at <https://pubs.acs.org/10.1021/jacs.1c11793>

### Funding

This work was supported by the National Science Centre (MC from grant SYMFONIA 2016/20/W/ST5/00478 and AS and PC from OPUS 2017/25/B/ST5/01011) add and the Wrocław Centre for Networking and Supercomputing (grant no. 299).

### Notes

The authors declare no competing financial interest.

## ACKNOWLEDGMENTS

We would like to thank Dr. Hanna Jędrzejewska (Institute of Organic Chemistry, Polish Academy of Sciences) for her involvement in theoretical calculation.

## REFERENCES

- (1) MacGillivray, L. R.; Atwood, J. L. A chiral spherical molecular assembly held together by 60 hydrogen bonds. *Nature* **1997**, *389*, 469–472.
- (2) Gerkensmeier, T.; Iwanek, W.; Avena, C.; Fröhlich, R.; Kotila, S.; Näther, C.; Mattay, J. Self-Assembly of 2,8,14,20-Tetraisobutyl-5,11,17,23-tetrahydroxyresorc[4]arene. *Eur. J. Org. Chem.* **1999**, 2257–2262.
- (3) (a) Wilson, C. F.; Eastman, M. P.; Hartzell, C. J. Hydrogen Bonding in a Host–Guest System: C-Undecylcalix[4]resorcinarene and Water in Benzene. *J. Phys. Chem. B* **1997**, *101*, 9309–9313. (b) Avram, L.; Cohen, Y. Spontaneous formation of hexameric resorcinarene capsule in chloroform solution as detected by diffusion

- NMR. *J. Am. Chem. Soc.* **2002**, *124*, 15148–15149. (c) Shivanyuk, A.; Rebek, J. Assembly of Resorcinarene Capsules in Wet Solvents. *J. Am. Chem. Soc.* **2003**, *125*, 3432–3433. (d) Yamanaka, M.; Shivanyuk, A.; Rebek, J. Kinetics and Thermodynamics of Hexameric Capsule Formation. *J. Am. Chem. Soc.* **2004**, *126*, 2939–2943. (e) Evan-Salem, T.; Baruch, I.; Avram, L.; Cohen, Y.; Palmer, L. C.; Rebek, J., Jr. Resorcinarenes are hexameric capsules in solution. *Proc. Natl. Acad. Sci. U.S.A.* **2006**, *103*, 12296–12300. (f) Cohen, Y.; Evan-Salem, T.; Avram, L. Hydrogen-Bonded Hexameric Capsules of Resorcin[4]arene, Pyrogallol[4]arene and Octahydroxypyridine[4]arene are Abundant Structures in Organic Solvents: A View from Diffusion NMR. *Supramol. Chem.* **2008**, *20*, 71–79.
- (4) (a) Shivanyuk, A.; Rebek, J., Jr. Reversible encapsulation by self-assembling resorcinarene subunits. *Proc. Natl. Acad. Sci. U.S.A.* **2001**, *98*, 7662–7665. (b) Shivanyuk, A.; Rebek, J., Jr. Reversible encapsulation of multiple, neutral guests in hexameric resorcinarene hosts. *Chem. Commun.* **2001**, 2424–2425. (c) Philip, I. E.; Kaifer, A. E. Electrochemically driven formation of a molecular capsule around the ferrocenium ion. *J. Am. Chem. Soc.* **2002**, *124*, 12678–12679. (d) Avram, L.; Cohen, Y. Effect of a cationic guest on the characteristics of the molecular capsule of resorcinarene: A diffusion NMR study. *Org. Lett.* **2003**, *5*, 1099–1102. (e) Avram, L.; Cohen, Y. Discrimination of guests encapsulation in large hexameric molecular capsules in solution: Pyrogallol[4]arene versus resorcin[4]arene capsules. *J. Am. Chem. Soc.* **2003**, *125*, 16180–16181. (f) Avram, L.; Cohen, Y. Self-assembly of resorcin[4]arene in the presence of small alkylammonium guests in solution. *Org. Lett.* **2008**, *10*, 1505–1508. (g) Yariv-Shoushan, S.; Cohen, Y. Encapsulated or Not Encapsulated? Ammonium Salts Can Be Encapsulated in Hexameric Capsules of Pyrogallol[4]arene. *Org. Lett.* **2016**, *18*, 936–939.
- (5) Avram, L.; Cohen, Y. Self-Recognition, Structure, Stability, and Guest Affinity of Pyrogallol[4]arene and Resorcin[4]arene Capsules in Solution. *J. Am. Chem. Soc.* **2004**, *126*, 11556–11563.
- (6) (a) Zhang, Q.; Tiefenbacher, K. Hexameric Resorcinarene Capsule is a Brønsted Acid: Investigation and Application to Synthesis and Catalysis. *J. Am. Chem. Soc.* **2013**, *135*, 16213–16219. (b) Zhang, Q.; Tiefenbacher, K. Terpene cyclization catalysed inside a self-assembled cavity. *Nat. Chem.* **2015**, *7*, 197–202. (c) Catti, L.; Tiefenbacher, K. Bronsted Acid-Catalyzed Carbonyl-Olefin Metathesis inside a Self-Assembled Supramolecular Host. *Angew. Chem., Int. Ed.* **2018**, *57*, 14589–14592. (d) Zhang, Q.; Catti, L.; Tiefenbacher, K. Catalysis inside the Hexameric Resorcinarene Capsule. *Acc. Chem. Res.* **2018**, *51*, 2107–2114. (e) Némethová, I.; Synttrivani, L.-D.; Tiefenbacher, K. Molecular Capsule Catalysis: Ready to Address Current Challenges in Synthetic Organic Chemistry? *Chimia* **2020**, *74*, 561–568.
- (7) (a) La Manna, P.; Talotta, C.; Floresta, G.; De Rosa, M.; Soriente, A.; Rescifina, A.; Gaeta, C.; Neri, P. Mild Friedel-Crafts Reactions inside a Hexameric Resorcinarene Capsule: C-Cl Bond Activation through Hydrogen Bonding to Bridging Water Molecules. *Angew. Chem., Int. Ed.* **2018**, *57*, 5423–5428. (b) Gambaro, S.; De Rosa, M.; Soriente, A.; Talotta, C.; Floresta, G.; Rescifina, A.; Gaeta, C.; Neri, P. A hexameric resorcinarene capsule as a hydrogen bonding catalyst in the conjugate addition of pyrroles and indoles to nitroalkenes. *Org. Chem. Front.* **2019**, *6*, 2339–2347. (c) Gambaro, S.; La Manna, P.; De Rosa, M.; Soriente, A.; Talotta, C.; Gaeta, C.; Neri, P. The Hexameric Resorcinarene Capsule as a Bronsted Acid Catalyst for the Synthesis of Bis(heteroaryl)methanes in a Nanoconfined Space. *Org. Chem. Front.* **2019**, *7*, 687. (d) La Manna, P.; De Rosa, M.; Talotta, C.; Rescifina, A.; Floresta, G.; Soriente, A.; Gaeta, C.; Neri, P. Synergic Interplay Between Halogen Bonding and Hydrogen Bonding in the Activation of a Neutral Substrate in a Nanoconfined Space. *Angew. Chem., Int. Ed.* **2020**, *59*, 811–818. (e) Gambaro, S.; Talotta, C.; Sala, P. D.; Soriente, A.; De Rosa, M.; Gaeta, C.; Neri, P. Kinetic and Thermodynamic Modulation of Dynamic Imine Libraries Driven by the Hexameric Resorcinarene Capsule. *J. Am. Chem. Soc.* **2020**, *142*, 14914–14923.
- (8) (a) La Sorella, G.; Sporni, L.; Strukul, G.; Scarso, A. Supramolecular Encapsulation of Neutral Diazoacetate Esters and Catalyzed 1,3-Dipolar Cycloaddition Reaction by a Self-Assembled Hexameric Capsule. *ChemCatChem* **2015**, *7*, 291–296. (b) Borsato, G.; Scarso, A. Catalysis within the Self-Assembled Resorcin[4]arene Hexamer. *Organic Nanoreactors*; Academic Press: London, 2016; pp 203–234. (c) Caneva, T.; Sporni, L.; Strukul, G.; Scarso, A. Efficient epoxide isomerization within a self-assembled hexameric organic capsule. *RSC Adv.* **2016**, *6*, 83505–83509.
- (9) Kumari, H.; Deakyn, C. A.; Atwood, J. L. Solution Structures of Nanoassemblies Based on Pyrogallol[4]arenes. *Acc. Chem. Res.* **2014**, *47*, 3080–3088.
- (10) (a) Rebek, J., Jr. Hexameric Capsules from Resorcinarenes and Pyrogallolarenes. *Hydrogen-Bonded Capsules: Molecular Behaviour in Small Spaces*; World Scientific Publishing Company, 2015; pp 99–115. (b) Zhu, Y.; Rebek, J., Jr.; Yu, Y. Cyclizations catalyzed inside a hexameric resorcinarene capsule. *Chem. Commun.* **2019**, *55*, 3573–3577.
- (11) Avram, L.; Cohen, Y.; Rebek, J., Jr. Recent advances in hydrogen-bonded hexameric encapsulation complexes. *Chem. Commun.* **2011**, *47*, 5368–5375.
- (12) (a) Gaeta, C.; Talotta, C.; De Rosa, M.; La Manna, P.; Soriente, A.; Neri, P. The hexameric resorcinarene capsule at work: supramolecular catalysis in confined spaces. *Chem.—Eur. J.* **2019**, *25*, 4899–4913. (b) Gaeta, C.; La Manna, P.; De Rosa, M.; Soriente, A.; Talotta, C.; Neri, P. Supramolecular Catalysis with Self-Assembled Capsules and Cages: What Happens in Confined Spaces. *ChemCatChem* **2020**, *13*, 1638–1658.
- (13) Chwastek, M.; Szumna, A. Higher Analogues of Resorcinarenes and Pyrogallolarenes: Bricks for Supramolecular Chemistry. *Org. Lett.* **2020**, *22*, 6838–6841.
- (14) Chwastek, M.; Cmoch, P.; Szumna, A. Dodecameric anion-sealed capsules based on pyrogallol[5]arenes and resorcin[5]arenes. *Angew. Chem., Int. Ed.* **2021**, *60*, 4540–4544.
- (15) Kantcheva, A. K.; Quick, M.; Shi, L.; Winther, A.-M. L.; Stolzenberg, S.; Weinstein, H.; Javitch, J. A.; Nissen, P. Chloride binding site of neurotransmitter sodium symporters. *Proc. Natl. Acad. Sci. U.S.A.* **2013**, *110*, 8489–8494.
- (16) Coleman, J. A.; Green, E. M.; Gouaux, E. X-ray structures and mechanism of the human serotonin transporter. *Nature* **2016**, *532*, 334–339.
- (17) (a) Smith, D. K. Rapid NMR screening of chloride receptors: uncovering catechol as a useful anion binding motif. *Org. Biomol. Chem.* **2003**, *1*, 3874–3877. (b) Winstanley, K. J.; Sayer, A. M.; Smith, D. K. Anion binding by catechols—an NMR, optical and electrochemical study. *Org. Biomol. Chem.* **2006**, *4*, 1760–1767.
- (18) Mansikkamäki, H.; Nissinen, M.; Rissanen, K. Encapsulation of diquats by resorcinarenes: a novel staggered anion–solvent mediated hydrogen bonded capsule. *Chem. Commun.* **2002**, 1902–1903.
- (19) Mansikkamäki, H.; Nissinen, M.; Schalley, C. A.; Rissanen, K. Self-assembling resorcinarene capsules: solid and gas phase studies on encapsulation of small alkyl ammonium cations. *New J. Chem.* **2003**, *27*, 88–97.
- (20) Beyeh, N. K.; Weimann, D. P.; Kaufmann, L.; Schalley, C. A.; Rissanen, K. Ion Pair Recognition of Tetramethyl Ammonium Salts by Halogenated Resorcinarenes. *Chem.—Eur. J.* **2012**, *18*, 5552–5557.
- (21) Beyeh, N. K.; Göth, M.; Kaufmann, L.; Schalley, C. A.; Rissanen, K. The synergistic interplay of weak interactions in the ion pair recognition of quaternary and diquaternary ammonium salts by halogenated resorcinarenes. *Eur. J. Org. Chem.* **2014**, *2014*, 80–85.
- (22) Avram, L.; Cohen, Y. Diffusion NMR of molecular cages and capsules. *Chem. Soc. Rev.* **2015**, *44*, 586–602.
- (23) Frisch, M. J.; Trucks, G. W.; Schlegel, H. B.; Scuseria, G. E.; Robb, M. A.; Cheeseman, J. R.; Scalmani, G.; Barone, V.; Petersson, G. A.; Nakatsuji, H.; Li, X.; Caricato, M.; Marenich, A. V.; Bloino, J.; Janesko, B. G.; Gomperts, R.; Mennucci, B.; Hratchian, H. P.; Ortiz, J. V.; Izmaylov, A. F.; Sonnenberg, J. L.; Williams-Young, D.; Ding, F.; Lipparini, F.; Egidi, F.; Goings, J.; Peng, B.; Petrone, A.; Henderson, T.; Ranasinghe, D.; Zakrzewski, V. G.; Gao, J.; Rega, N.; Zheng, G.; Liang, W.; Hada, M.; Ehara, M.; Toyota, K.; Fukuda, R.; Hasegawa, J.; Ishida, M.; Nakajima, T.; Honda, Y.; Kitao, O.; Nakai, H.; Vreven, T.; Throssell, K.; Montgomery, J. A., Jr.; Peralta, J. E.; Ogliaro, F.; Bearpark,



M. J.; Heyd, J. J.; Brothers, E. N.; Kudin, K. N.; Staroverov, V. N.; Keith, T. A.; Kobayashi, R.; Normand, J.; Raghavachari, K.; Rendell, A. P.; Burant, J. C.; Iyengar, S. S.; Tomasi, J.; Cossi, M.; Millam, J. M.; Klene, M.; Adamo, C.; Cammi, R.; Ochterski, J. W.; Martin, R. L.; Morokuma, K.; Farkas, O.; Foresman, J. B.; Fox, D. J. Gaussian 09, Revision E.01; Gaussian, Inc.: Wallingford CT, 2016.

(24) (a) Zhang, C.; Patil, R. S.; Atwood, J. L. Metallosupramolecular Complexes Based on Pyrogallol[4]arenes. *Advances in Inorganic Chemistry*; Elsevier: Amsterdam, 2018, pp 247–276. (b) Dalgarno, S. J.; Power, N. P.; Atwood, J. L. Metallo-supramolecular capsules. *Chem. Rev.* **2008**, *252*, 825–841. (c) Jin, P.; Dalgarno, S. J.; Atwood, J. L. Mixed metal-organic nanocapsules. *Coord. Chem. Rev.* **2010**, *254*, 1760–1768.

(25) Wu, B.; Jia, C.; Wang, X.; Li, S.; Huang, X.; Yang, X.-J. Chloride Coordination by Oligoureas: From Mononuclear Crescents to Dinuclear Foldamers. *Org. Lett.* **2012**, *14*, 684–687.

(26) Szymański, M.; Wierzbicki, M.; Gilski, M.; Jędrzejewska, H.; Sztylko, M.; Cmoch, P.; Shkurenko, A.; Jaskólski, M.; Szumna, A. Mechanochemical Encapsulation of Fullerenes in Peptidic Containers Prepared by Dynamic Chiral Self-Sorting and Self-Assembly. *Chem.—Eur. J.* **2016**, *22*, 3148–3155.

(27) Szymański, M. P.; Jędrzejewska, H.; Wierzbicki, M.; Szumna, A. On the mechanism of mechanochemical molecular encapsulation in peptidic capsules. *Phys. Chem. Chem. Phys.* **2017**, *19*, 15676–15680.

(28) Journey, S. N.; Teppang, K. L.; Garcia, C. A.; Brim, S. A.; Onofrei, D.; Addison, J. B.; Holland, G. P.; Purse, B. W. Mechanically induced pyrogallol[4]arene hexamer assembly in the solid state extends the scope of molecular encapsulation. *Chem. Sci.* **2017**, *8*, 7737–7745.

(29) Jędrzejewska, H.; Wielgus, E.; Kaźmierski, S.; Rogala, H.; Wierzbicki, M.; Wróblewska, A.; Pawlak, T.; Potrzebowski, M. J.; Szumna, A. Porous Molecular Capsules as Non-Polymeric Transducers of Mechanical Forces to Mechanophores. *Chem.—Eur. J.* **2020**, *26*, 1558–1566.

(30) Williamson, M. P. Using chemical shift perturbation to characterise ligand binding. *Prog. Nucl. Magn. Reson. Spectrosc.* **2013**, *73*, 1–16.

(31) Horiuchi, S.; Matsuo, C.; Sakuda, E.; Arikawa, Y.; Clever, G. H.; Umakoshi, K. Anion-mediated encapsulation-induced emission enhancement of an IrIII complex within a resorcin[4]arene hexameric capsule. *Dalton Trans.* **2020**, *49*, 8472–8477.